Contents lists available at SciVerse ScienceDirect

Biochimica et Biophysica Acta

journal homepage: www.elsevier.com/locate/bbamem

Enforcing the positive charge of N-termini enhances membrane interaction and antitumor activity of bovine seminal ribonuclease

Gerardino D'Errico [a,b], Carmine Ercole [a], Marisa Lista [a], Elio Pizzo [c], Annarita Falanga [d], Stefania Galdiero [d,e], Roberta Spadaccini [a,f], Delia Picone [a,*]

[a] Dipartimento di Chimica "Paolo Corradini", Università degli Studi di Napoli "Federico II", Via Cintia, 80126 Napoli, Italy
[b] CSGI, Consorzio interuniversitario per lo sviluppo dei Sistemi a Grande Interfase, Italy
[c] Dipartimento di Biologia Strutturale e Funzionale, Università degli Studi di Napoli "Federico II", Via Cintia, 80126 Napoli, Italy
[d] Dipartimento di Scienze Biologiche, Università degli Studi di Napoli "Federico II", Via Mezzocannone 16, 80134 Napoli, Italy
[e] Istituto di Biostrutture e Bioimmagini, CNR, Via Mezzocannone 16, 80134 Napoli, Italy
[f] Dipartimento di Scienze Biologiche ed Ambientali, Università del Sannio, Via Port'Arsa 11, 82100 Benevento, Italy

ARTICLE INFO

ABSTRACT

Binding to cell membrane, followed by translocation into the cytosol and RNA degradation, is a necessary requirement to convert a ribonuclease into a cytotoxin for malignant tumor cells. In this paper, we investigate the membrane binding attitude of bovine seminal ribonuclease (BS-RNase) and its variant G38K-BS-RNase, bearing an enforced cluster of positive charges at the N-termini surface. By using a combination of biophysical techniques, including CD, SPR and ESR, we find for the two proteins a common, two-step mechanism of interaction with synthetic liposomes, an initial binding to the bilayer surface, driven by electrostatic interactions, followed by a shallow penetration in the lipid core. Protein binding effectively perturbs lipid packing and dynamics. Remarkably, the higher G38K-BS-RNase membrane interacting capability well correlates with its increased cytotoxicity for tumor cells. Overall, these studies shed light on the mechanism of membrane binding and perturbation, proving definitely the importance of electrostatic interactions in the cytotoxic activity of BS-RNase, and provide a rational basis to design proteins with anticancer potential.

© 2011 Elsevier B.V. All rights reserved.

1. Introduction

The central role of RNA in the regulation of many vital processes, occurring under both physiological and pathological conditions, has emerged clearly over the past 10 years (for a very recent review see [1]. As a consequence, most ribonucleases have received a considerable interest for their association with health and diseases, including human cancer development [2], and are considered potential targets for drug design [3] because of their strong cytotoxic activity toward malignant tumor cells. One of the enzymes of this class, the amphibian Onconase, reached also clinical trials [4]. Different RNAs are degraded by these proteins, whose antitumor activity is critically dependent on a complex series of biochemical events, involving interactions with different cellular compartments. The crucial steps of this process include binding to negatively charged cell membrane, translocation into the cytosol via endocytosis [5] and RNA degradation. Furthermore, to fully exploit their antitumor potential, ribonucleases have to resist to protease attack and to evade Ribonuclease Inhibitor [6], a 50 kDa horse-shoe shaped protein that binds with very high affinity most monomeric ribonucleases and hampers their activity [7]. Previous structure-activity relationship studies allowed the identification of the crucial features that these enzymes have to fulfill to exhibit antitumor activity: i) a strong positive surface potential to allow membrane interaction; ii) a functional catalytic site and iii) a 3D structure able to evade Ribonuclease Inhibitor.

In principle, it is possible to increase the antitumor potentiality of ribonucleases by chemical modifications or protein engineering but until now this target remained essentially elusive. Enforcing the cytotoxicity by influencing the enzymatic activity is not straightforward;

indeed, while the presence of a functional catalytic site is required, there is no direct correlation between catalytic efficiency and antitumor potentiality [8]. On the other hand, the enhancement of RI resistance is more feasible, since RNase A and human pancreatic ribonuclease variants designed to avoid binding were found to be cytotoxic [9,10]. Strategies to enhance ribonucleases ability to evade RI have been inspired by naturally occurring antitumor ribonucleases, which avoid binding because either they lack residues directly involved in the complex with RI, like in the case of Onconase, or their 3D structure does not allow the formation of a stable complex with RI. This has a paradigmatic example in bovine seminal ribonuclease (BS-RNase) [11], which shows antitumor activity *in vitro* and on model animals [12]. BS-RNase is a dimeric protein constituted by two identical subunits covalently linked through two disulfide bridges (for a review, see [7]); it is isolated as an equilibrium mixture of two isoforms, with or without exchange (swapping) of the N-termini, indicated as MxM and M=M respectively [13]. X-ray structures [14,15] revealed that the two isoforms present only minor differences in their tertiary structure, located essentially at level of 16–22 hinge region, *i.e.* the loop connecting the dislocating extremity to the protein body. However, under reducing conditions, the two isoforms behave differently: the swapped form, being converted into a so-called non-covalent dimer (NCD), still evades RI binding [16], whilst the unswapped one dissociates into two monomers, which are inactivated by RI. Thus, it could be hypothesized that an increasing of the MxM fraction with respect to M=M should result in an increased ability to evade RI and, consequently, in a higher antitumor activity. However, we have obtained enzymatically active BS-RNase variants with the same swapping amount of the native protein but a very low antitumor activity [17], suggesting that the swapping *per se* is not sufficient to elicit the antitumor activity, and making the relationships between swapping and cytotoxicity still complicated.

As last strategy to enhance ribonucleases antitumor activity one could act on their internalization efficiency, relying on the pieces of evidence that ribonucleases directly injected into the cytosol are more toxic than those added to cells externally [18]. Also in this case, natural ribonucleases are useful templates for protein engineering. A correlation with the number of positive charges on the protein surface and the cytotoxic activity has been already reported for several vertebrate ribonucleases, including Onconase [19], RNase A oligomers [20] and BS-RNase [21]. Particularly, in comparison with RNase A, the higher pI of BS-RNase enhances the interaction with phospholipid membranes and allows a better internalization [22]. In addition, based on *in silico* studies, it has been proposed that the BS-RNase face interacting with membrane is the one hosting the N-termini (henceforth designed N-face) which, in the native protein, is characterized by a large positive potential that promotes a strong interaction with the negatively charged phospholipids of the cellular membrane [21]. However, this hypothesis has not been experimentally proved so far.

Based on these premises, in this paper we have explored the possibility to strengthen the antitumor activity of BS-RNase by improving the protein/membrane through the enhancement of the positive potential of this same surface, *i.e.* we have produced the G38K-BS-RNase variant (henceforth called G38K), and found that it shows a higher cytotoxicity toward tumor cells. Since this variant does not present any change both in the catalytic activity and in the ability to evade RI, we hypothesized the higher cytotoxicity to be connected to its enhanced interaction with membranes. To support this idea, we performed a detailed investigation of the membrane interaction process of BS-RNase and G38K with synthetic liposomes by using a combination of biophysical techniques. These studies shed light on the mechanism of membrane interaction, proving definitely the importance of electrostatic interactions in the cytotoxic activity toward tumor cells, and can be helpful to design proteins with even improved antitumor potentiality.

2. Materials and methods

2.1. Homology modeling and electrostatic potential calculation

The homology model of the G38K variant was calculated upon the crystal structure of the swapped BS-RNase (pdb code 1BSR) using Modeller 8v5 program [23]. The quality of the structural models was evaluated with the same program using the score of variable target function method [24]. Model analyses were performed using MOLMOL [25] and PyMOL [26]. The electrostatic potential was calculated using the program MGLTools-PMV.

2.2. Determination of electrostatic energy of interaction with charged membranes

The orientation-dependent electrostatic free energy due to the presence of a uniform electrostatic field generated by a charged membrane was computed by solving the Poisson-Boltzmann equation using the program DELPHI4 [27]. Similar to the modeling study of Notomista et al. [21] we assumed a surface charge density of 192 negative charges distributed over an area of 117×108 Å^2, which results in a strong uniform electrostatic field of 0.352×10^9 V/m in the direction of the z-axis. The dimer was placed at a distance of 55 Å from the membrane, in order to avoid close contacts which are difficult to describe with a continuum model. The molecule was then rotated in steps of 30° around the z-axis. For each rotation a second rotation around the x-axis in steps of 30° was applied. A third rotation around the z-axis should be applied to complete the rotational space sampling. This was not done because of the symmetry of the applied electric field.

2.3. Protein samples

The QuikChange Site-Directed Mutagenesis Kit protocol (Stratagene, La Jolla, CA) was used to substitute glycine 38 with lysine (G38K) in pET-22b(+) plasmid cDNA coding for BS-RNase, already available in our laboratory, which contained the N67D substitution to avoid local heterogeneity arising from the spontaneous deamidation occurring at position 67 [28,29].

The monomeric derivatives of BS-RNase and its G38K variant were expressed in *E. coli* cells and purified as previously described [30,31], with cysteines 31 and 32 linked to two glutathione molecules. Once assessed the purity of the protein samples and the correctness of their fold by gel-electrophoresis, CD and 2D NMR analysis, the enzymatic activity on yeast RNA was evaluated as usual [32] and found very close to each other for the two proteins, and also close to the literature data. The monomers were converted in the corresponding dimers following the procedure already reported [33]; as usual, the main product at the first purification step was the unswapped dimer. The protein solutions were then incubated at 37 °C to allow the conformational equilibrium between swapped and unswapped isoforms; the swapping extent was then assessed by two independent methods, as reported before [34], and found about 70% for both the recombinant proteins, as in native BS-RNase. Also for the dimeric form of G38K the enzymatic activity on yeast RNA was found very close to that of the parent BS-RNase.

2.4. Cytotoxicity studies

Before the cytotoxicity assays, the N-terminal methionine was removed with *Aeromonas proteolytica* aminopeptidase (Sigma) [35].

Cytotoxicity of BS-RNase and G38K was evaluated by performing the 3-(4,5-Dimethylthiazol-2-yl)-2,5-diphenyltetrazolium bromide (MTT) reduction inhibition assay [36]. Simian-virus-40-transformed mouse fibroblasts (SVT2 cells) and the parental non transformed Balb/C 3T3-line (3T3 cells) were obtained from the A.T.C.C. (American Type Culture

Collection, Manassas, VA, U.S.A.) and grown in Dulbecco's Modified Eagle's medium (DMEM) supplemented with 10% fetal bovine serum, 4 mM glutamine, 400 units/ml penicillin and 0.1 mg/ml streptomycin. Cell lines were maintained at 37 °C in a humidified incubator containing 5% CO_2. The cells were plated on 96-well plates at a density of 2.5×10^3 cells/well in 100 μl of medium containing either BS-RNase or the G38K variant up to a final protein concentration of 25, 50 and 100 μg/ml, corresponding to 0.9, 1.8 and 3.6 μM respectively. After 24, 48 and 72 h of incubation, 10 μl of a 5 mg/ml stock MTT solution in PBS, corresponding to a final concentration of 0.5 mg/ml in DMEM (final volume 100 μl), were added to the cells. After incubation of 4 h the MTT solution was removed and the MTT formazan salts were dissolved in 100 μl of 0.1 N HCl in anhydrous isopropanol. Cell survival is expressed as the absorbance of blue formazan measured at 570 nm with an automatic plate reader (Victor3 Multilabel Counter, Perkin Elmer, Shelton, CT).

2.5. CD spectra measurements and check of the protein stability vs. T

The CD spectra were recorded with a Jasco J-715 spectropolarimeter equipped with a Peltier type temperature control system (Model PTC-348WI). A protein concentration of about 0.3 mg ml^{-1} (about 10.8 μM) in 10 mM sodium acetate buffer, pH 5.0, was used. Thermal unfolding curves were recorded in the temperature scan mode at 222 nm from 25 up to 85 °C with a scan rate of 1.0 °C min^{-1}. For each protein sample, T_m vas calculated by nonlinear regression analysis of the experimental data, as the value corresponding to the midpoint of the denaturation curve. The full reversibility of thermal transition was assessed by CD for all proteins, since the CD curves were completely recovered upon cooling the protein solutions at room temperature. CD spectra and thermal denaturation measurements were acquired also in the presence of dimyristoyl phosphatidylglycerol (DMPG) large unilamellar vesicles (LUVs, see Section 2.6) using a protein/phospholipid ratio 1:100 w/w.

2.6. Phospholipid bilayer preparation

To experimentally study the interaction between proteins and lipid membranes, SPR, ESR and CD experiments were performed on BS-RNase or G38K in the presence of bilayers formed by dilauroyl phosphatidylglycerol (DLPG), in the form of supported bilayers (for SPR measurements) or liposomes (for ESR and CD measurements). Bilayers to be used for ESR measurements also included 1% w/w of spin-labeled phosphatidylcholines (n-PCSL) with the nitroxide group at different positions, n, in the sn-2 acyl chain. DLPG and spin-labels were obtained from Avanti Polar Lipids (Birmingham, AL, USA) and used without further purification.

Phospholipid liposomes were prepared by dissolving the lipids in a CHCl$_3$/MeOH mixture (2/1 v/v). The solvents were then evaporated under a stream of nitrogen, and the lipids were subjected to a vacuum for at least 3 h and then resuspended in sodium acetate buffer 10 mM pH 5.0 by vortexing. The resulting dispersions contained multilamellar vesicles (MLVs) that were used as such for ESR experiments. To perform CD measurements, large unilamellar vesicles (LUVs), preferred for their lower scattering, were obtained from MLVs by extrusion 11 times through polycarbonate membranes with 0.1 μm diameter pores. In the case of SPR experiments, supported lipid bilayer were prepared starting from small unilamellar vesicles (SUVs) prepared by sonication of MLVs, following the protocol previously described [37].

2.7. Binding analysis to liposomes by surface plasmon resonance (SPR).

SPR experiments were carried out with a BIAcore 3000 analytical system (Biacore, Uppsala, Sweden) using the L1 sensor chip and an experimental protocol previously described by Mozsolits et al. [38].

The running buffer used for all experiments was sodium acetate 10 mM pH 5.0; the washing solution was 40 mM N-octyl β-D-glucopyranoside (25 μl, 5 μl/min). All solutions were freshly prepared, degassed, and filtered through 0.22 μm pores. DLPG SUVs (80 μl, 0.5 mM) were then applied to the chip surface at a flow rate of 2 μl/min at a temperature of 25 °C. To remove any multilamellar structures from the lipid surface, we used NaOH 10 mM and increased the flow rate to 50 μl/min, which resulted in a stable baseline corresponding to the lipid bilayer linked to the chip surface. The negative control BSA was injected (25 μl, 0.1 mg/μl in sodium acetate buffer) to confirm complete coverage of the nonspecific binding sites. A range of contact times and flow rates have been examined. BS-RNase and G38K solutions (200 μl, 600 s) were injected onto the lipid surface at a flow rate of 20 μl/min to avoid limitation by mass transfer. On completion of injection, buffer flow continued for 15 min to allow protein dissociation. A sensorgram was obtained by plotting the SPR angle against time. This change in the angle is then translated to response units and the protein-lipid binding event was characterized from a series of sensorgrams collected at different protein concentrations (5 nM–50 nM).

The sensorgrams were analyzed by curve fitting using numerical integration analysis [39]. The BIAevaluation routine was used to perform complete kinetic analyses of the peptide sensorgrams. Several curve fitting algorithms were used but good fit was obtained only with the two-state reaction model, which was previously used for describing the possible binding mechanisms of antimicrobial peptides. The data were fitted globally by simultaneously fitting the sensorgrams obtained at different protein concentrations and the two-state reaction model was applied to each dataset. This model [38] describes two reaction steps:

$$P + L \underset{kd1}{\overset{Ka1}{\rightleftharpoons}} PL \underset{kd2}{\overset{ka2}{\rightleftharpoons}} PL^*$$
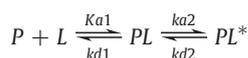
The two steps may correspond to the protein (P) binding to lipids (L) to give PL and to the complex PL changing to PL*, which cannot dissociate directly to P+L and which may correspond to partial insertion of the protein into the lipid bilayer. The corresponding differential rate equations for this reaction model are:

$$dRU_1/dt = k_{a1} \times C_A \times (RU_{max} - RU_1 - RU_2) - k_{d1} \times RU_1 - k_{a2} \times RU_1$$
$$+ k_{d2} \times RU_2 dRU_2/$$
$$dt = k_{a2} \times RU_1 - k_{d2} RU_2$$

where RU1 and RU2 are the response units for the first and second steps, respectively, CA is the protein concentration, RU$_{max}$ is the maximum protein binding capacity (or equilibrium binding response), and k_{a1}, k_{d1}, k_{a2}, and k_{d2} are the association and dissociation rate constants for the first and second steps, respectively.

While k_{a1} has M^{-1} s^{-1} units, k_{d1}, k_{a2}, and k_{d2} have s^{-1} units; thus the total affinity constant for the all process, K$_A$, has M^{-1} units. Kinetic data were assessed by using χ^2 values, plots of the residuals from the model fitting and the significance of a parameter assessed by standard deviations. The quality of the fit to a specific parameter was deemed significant if the standard deviation was less than 10%.

2.8. Electron spin resonance spectroscopy

Samples for ESR spectroscopy were prepared by mixing in small test tubes appropriate amounts of lipid in dichloromethane/methanol (2/1 v/v) and spin-labeled phosphatidylcholines in ethanol, following the procedure described above. The proteins were dissolved in the sodium acetate buffer 10 mM, pH 5.0, used to re-hydrate the lipid sample, mixed with the lipid solutions (typical volume 30–50 μl), heated above the lipid phase transition temperature with intermittent vortexing, and finally transferred to a 25 μL glass capillary.

ESR spectra were recorded on a 9-GHz Bruker Elexys E-500 spectrometer, at 25 °C, using procedures and instrument setting reported in literature [40].

In order to quantitatively analyze the spectra, the order parameter, S, and the isotropic nitrogen hyperfine coupling constant, a_N', were calculated according to a well-established model reported in the literature [41]. Values of the phenomenological hyperfine splitting parameters necessary to apply the model were determined by a home-made MATLAB-based routine, that fits the maxima and minima in the outer wings of a spectrum empirically to a Gaussian curve and calculates the field difference between the extrema [42]. Uncertainty on ESR parameters was estimated by evaluating their values for independently prepared samples with the same nominal composition.

3. Results and discussion

3.1. Rational protein design

In order to produce a variant with an increased positive potential at the N terminus region, without altering the fold and the activity of the BS-RNase, we have inspected the N-face of the protein, which has already a strong positive potential and, for this reason, has been supposed to represent the membrane-interacting face of the protein [21]. To enhance this positive potential, we decided to mutate a well exposed surface residue, glycine 38, to a lysine. The homology model of the G38K variant based on the crystal structure of the swapped dimer of BS-RNase (1BSR) confirmed a very close similarity among the two proteins. We compared also the electrostatic potential at the solvent accessible surfaces of G38K and BS-RNase and found, as expected, a strong polarity with a positive potential located at the N-terminus side in both cases but, as illustrated in Fig. 1A, the introduction of a basic residue at position 38 in the G38K variant creates an almost continuous patch of positive charges spanning from K39 of one subunit to K39 of other one, which includes also the two K1 residues. This feature is expected to increase the membrane binding capability.

We have then calculated the electrostatic interaction energy (EIE) between wild type BS-RNase and its G38K variant and negatively charged model membrane made of DMPG lipids assembled as previously reported in Notomista et al. [21]. A series of EIE values were calculated by varying the orientation of each RNase toward the membrane. The results of these calculations revealed that, for both BS-RNase and G38K, a single highest negative value of EIE could be
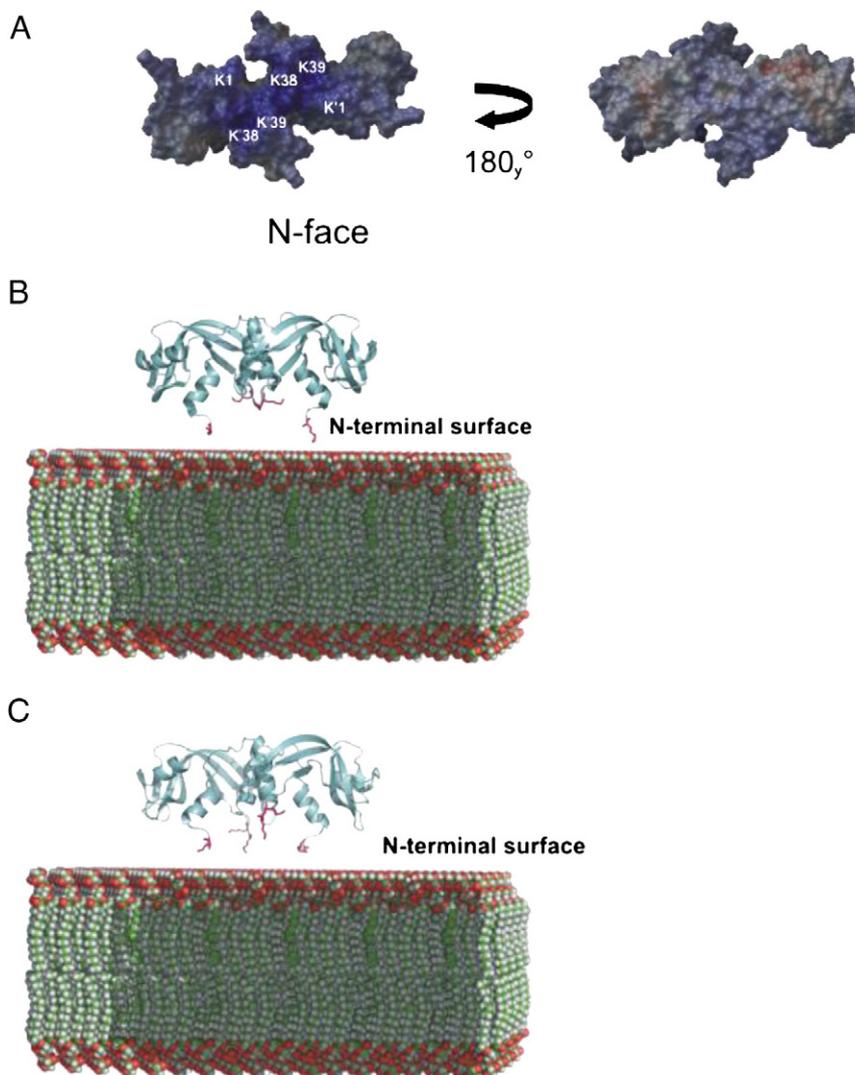

Fig. 1. (A) Electrostatic surface of the G38K. (B) Structure of the BS-RNase model membrane complex with the highest negative EIE value. Lipids are shown as van der Waals spheres and colored according to the atom type. (C) Structure of the G38K model membrane complex with the highest negative EIE value. Lipids are shown as van der Waals spheres and colored according to the atom type.

estimated. The strongest electrostatic interaction for both proteins is when the N-terminus region of the proteins is oriented toward the membrane (Fig. 1B and C). G38K has a better interaction with the membrane compared to BS-RNase, indeed the lowest value of interaction energy for G38K is about 20 kcal/mol below the corresponding one of BS-RNase. This difference suggests that electrostatics is important for the interaction with the membrane and that the G38K substitution may improve this interaction. On the basis of these data we decided to insert this mutation in the construct coding for BS-RNase.

3.2. Biochemical properties

The cytotoxic activity of BS-RNase and G38K was evaluated by measuring the proliferation of malignant SVT2 fibroblasts, both in dose-dependent and time-dependent assays. The results are illustrated in Fig. 2, reporting the cell survival after 24, 48 and 72 h of incubation following the protein addition. The curves indicate that in all the experimental conditions examined G38K displays a stronger cytotoxic activity, the percentage of cell survival being always lower than in the presence of the same amount of the parent BS-RNase. The cytotoxic activity is quite small after 24 h of incubation, the cell survival remaining in all conditions above 50%, and even the difference between the two proteins is not very evident: as an example, upon addition of 50 μg/ml of protein, the cell survival in the presence of G38K is only 15% lower than that observed with the parent BS-RNase. The different effect of the two proteins is more evident after 48 and 72 h when cell survival in presence of G38K is 65 and 70% lower than with BS-RNase. Furthermore, after 48 h there is a more clear dose dependent effect for both proteins, the percentage of alive cells being below 20% in the presence of 50 μg/mL of G38K and about 40% in the presence of the same amount of BS-RNase. Finally, after 72 h, a maximum of 15% of cell survival with respect to the untreated cells is observed with G38K, even in the presence of the lowest protein concentration utilized in this assay, i.e. 0.9 μM, while BS-RNase shows still a dose dependent activity. As expected, when assayed in the same experimental conditions, both proteins have no effects on the normal 3T3 cells (data not shown).

It is worth to recall here that an increased cytotoxic activity with respect to BS-RNase was obtained by Raines and coworkers [43] with the G38K/K39G/G88R-BS-RNase variant, which displayed antitumor activity even at monomeric state, due to a better resistance of the monomeric derivative to inhibition by RI [43]. However the authors attributed this property to the steric encumbrance of R88, which hinders the contact with W259 of RI, and to the abolition of the electrostatic interaction between K39 and E297 observed in the RNase A/RI complex [44], therefore the specific influence of the G38K substitution could not be isolated. Therefore, we decided to investigate the molecular basis of the cytotoxic activity of BS-RNase and its G38K variant, focusing on the mechanism of interaction with models of phospholipid membranes.

3.3. Circular dichroism spectra

It is well known from literature data that pancreatic-like ribonucleases are very stable proteins, with melting temperatures above 50 °C. Anyhow, to rule-out side-effects on the protein conformation and stability following liposome interaction, we have checked the BS-RNase and G38K conformation by Circular Dichroism studies in a wide temperature range (25–85 °C). CD thermal denaturation curves, acquired as described in detail in the experimental section, proved that both the proteins were completely stable around physiological temperatures, with T_m of 62 °C for BS-RNase and 60 °C for G38K. Furthermore, their conformation is not affected by liposomes, as no substantial differences in CD spectra or T_m were detected in the presence of DMPG liposomes. CD spectra at 25 °C of both the proteins
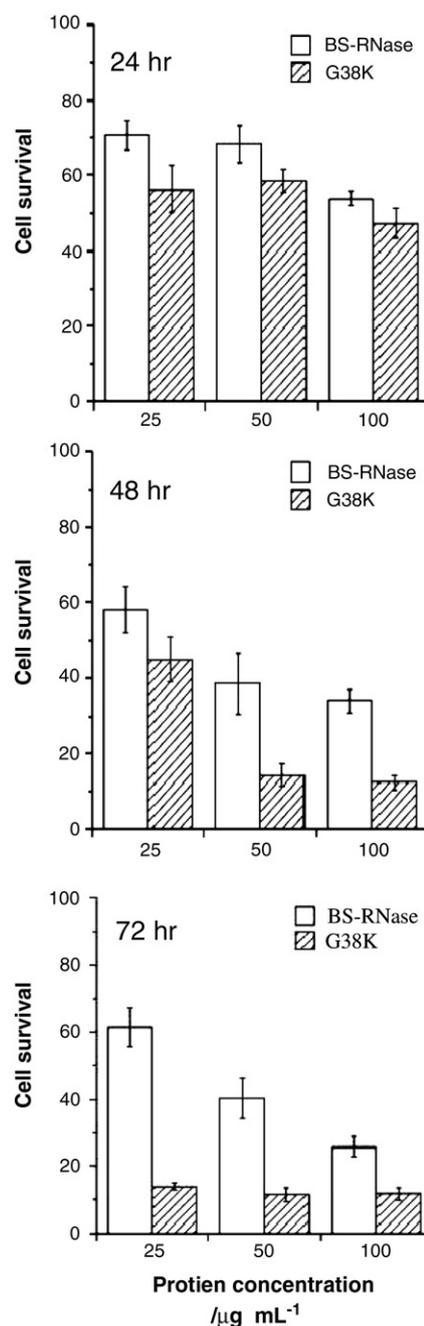

Fig. 2. Effects of RNase on the proliferation of murine malignant SVT2 fibroblasts. Cells, after a preliminary incubation for 24 h at 37 °C, were subjected to the presence of different amounts (25, 50 and 100 μg/L, corresponding to 0.9, 1.8 and 3.6 μM respectively) of BS-RNase and G38K for 24 h, 48 h and 72 h. Each value is the mean of at least three determinations and is expressed as percentage of the control, in which cells were grown in the absence of RNases.

with and without liposomes are reported in the Supporting Material (Fig. S1).

3.4. Membrane binding

We used the Biacore biosensor method to investigate the interaction between BS-RNase or its G38K variant with lipid bilayers. Since our modeling studies have shown that the driving force of this interaction is essentially electrostatic, we decided to use an anionic lipid, DLPG. Dilauroyl phospholipids, which are in the fluid state at 25 °C, have shown to be a good option for studies conducted around room temperature [42]. DLPG bilayers were absorbed onto the L1 chip.

Sensorgrams of the binding of the two proteins are shown in Fig. 3. The sensorgrams reveal that the RU signal intensity increases as a function of the protein concentration. This indicates that the amount of protein bound to liposomes is proportional to the protein concentration. The sensorgrams of the binding of the native protein compared to the variant show markedly lower response levels, indicating a stronger binding to liposomes of the variant protein (maximum concentration for G38K is 20 nM, while for BS-RNase is 50 nM). The inspection of the shape of each sensorgram reveals that the proteins bind to the lipid surfaces in a biphasic manner, with a more evident effect for the native protein. The initial association starts as a fast process and then slows down considerably toward the end of the injection. Moreover, the sensorgrams do not return to zero, indicating that the proteins remained significantly bound to the surface or inserted into the bilayer membrane.

We employed numerical integration analysis that uses nonlinear analysis to fit an integrated rate equation directly to the sensorgrams [45]. When fitting the protein's sensorgrams globally (using different concentrations of the protein) with the simplest 1:1 Langmuir binding model, a poor fit was obtained ($\chi^2 > 100$), confirming that this model does not represent the lipid binding mechanism. However, a significantly improved fit was obtained using numerical integration of the two-state reaction model of the binding sensorgrams, suggesting that there is likely to be at least two steps involved in the interaction between the protein and the bilayer. In analogy with previous studies of peptide-membrane interactions using SPR [46–48], the first step may correspond to the actual binding of the protein to the surface, and the second step to the insertion of the protein into the hydrophobic core of the membrane.
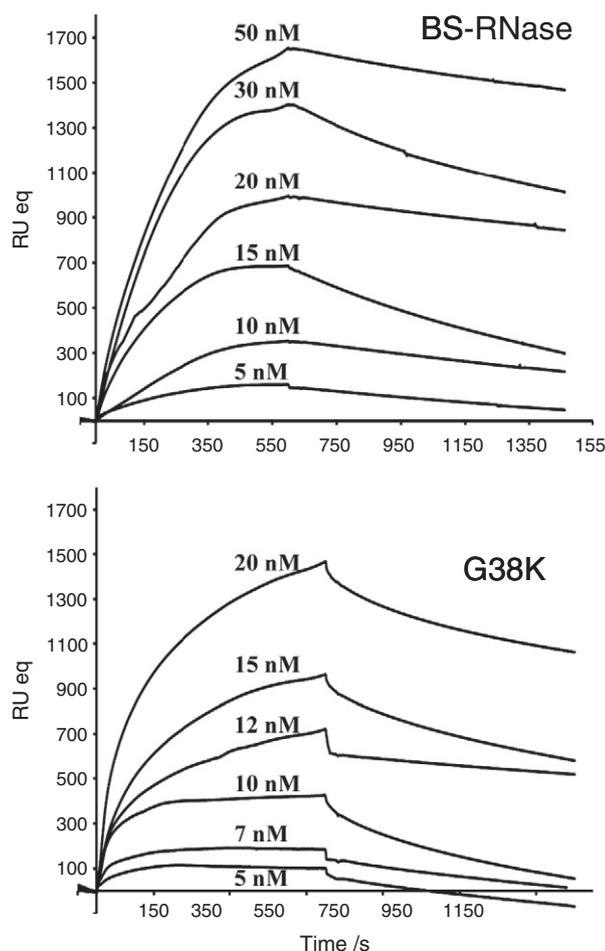

Fig. 3. Sensorgrams for the binding of BS-RNase and G38K with DLPG bilayers (L1 chip).

A set of protein sensorgrams with different protein concentrations was used to estimate the kinetic parameters. In this model, the values of k_{a1}/k_{d1} and k_{a2}/k_{d2} correspond to the affinity constants for electrostatic interaction and hydrophobic interaction, respectively. The average values for the rate constants obtained from the two-state model analysis are listed in Table 1 along with the affinity constant values (K_A). These data clearly indicate the main influence on the overall binding constant of the fast association rate and slow dissociation rate of the first step. If this step corresponds to the electrostatic interaction, these results clearly confirm that electrostatic forces play an important role in the binding of the protein. The higher affinity constants obtained for G38K is the result of an enhancement of the first step and not of the second step. This is because G38K binds approximately 10 fold faster (k_{a1}) to DLPG in the first step, while the binding rate constants are lower in the second step for both proteins. This indicates that the major difference between BS-RNase and G38K is in the initial contact with the bilayer and thus mainly in the electrostatic interaction.

3.5. Membrane interaction

SPR results not only point out the relevance of the initial adsorption of BS-RNase or G38K on the bilayer surface, essentially driven by electrostatic interactions, but also indicate that in the following step both proteins are inserted, at least partially, in the bilayer hydrophobic core. This point is worth to be investigated in more detail. Indeed, perturbation of the lipid packing represents the early stage of protein internalization, regardless of the specific membrane translocation mechanism. For this reason, we performed an ESR investigation on the association of BS-RNase and its variant with lipid membranes analyzing the perturbation of the chain mobility of spin-labeled phospholipids [49].

To investigate the depth of penetration of BS-RNase variants into the anionic phospholipid bilayer, we studied the perturbation that is induced by binding of BS-RNase or G38K on the ESR spectra of spin labels at different positions, n, in the sn-2 chain of the lipid. Fig. 4A gives the ESR spectra of the n-PCSL phosphatidylcholine spin-label positional isomers incorporated in DLPG bilayer membranes, in the presence and absence of either BS-RNase or G38K at a protein/lipid ratio of 1/1 (w/w). In the absence of proteins, the spectrum anisotropy decreases progressively with increasing n, as the spin-label position is stepped down the chain toward the center of the membrane, a characteristic hallmark of the liquid-crystalline state of fluid phospholipid bilayers (see, e.g., ref. [40]).

In the presence of BS-RNase, significant perturbations of the spectra of spin-labeled phospholipids are observed, due to a protein/liposome interaction. With respect to the spectra registered in the absence of the proteins, differences are more evident for G38K than for BS-RNase, according to an enhanced bilayer perturbation. For both proteins, differences become less evident with increasing n, i.e., for more internal spin-labels.

To quantitatively analyze these results we determined the order parameter of lipid acyl chains, S, and the nitrogen hyperfine coupling constant, a_N', which is an index of the micropolarity experienced by the nitroxide label [47]. Both a_N' and S decrease progressively with

Table 1
Association (k_{a1}, k_{a2}) and dissociation (k_{d1}, k_{d2}) rate constants obtained for the L1 chip using the two state model.

	k_{a1} ($M^{-1}s^{-1}$)	k_{d1} (s^{-1})	k_{a2} (s^{-1})	k_{d2} (s^{-1})	K_A (nM^{-1})
BS-RNase	(9.80 ± 0.04) 10^4	(2.07 ± 0.09) 10^{-3}	(4.90 ± 0.03) 10^{-2}	(2.76 ± 0.01) 10^{-2}	0.131
G38K	(6.80 ± 0.09) 10^5	(1.22 ± 0.03) 10^{-2}	(8.36 ± 0.02) 10^{-3}	(1.55 ± 0.05) 10^{-3}	0.355

The affinity constant (K_A) determined as $(k_{a1}/k_{d1}) \times (k_{a2}/k_{d2})$ is for the complete binding process.

increasing n, see Fig. 4B and C. The a_N' values are only marginally affected by the proteins. Perusal of Fig. 4B suggests that G38K and, to a minor extent, BS-RNase, increase the polarity experienced by the label
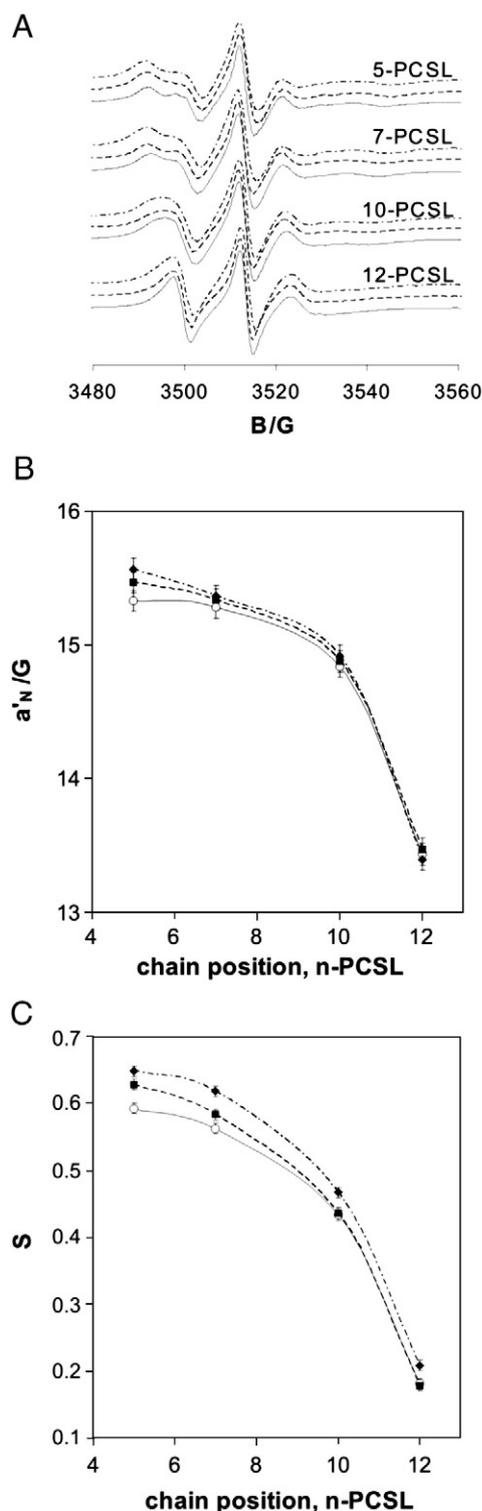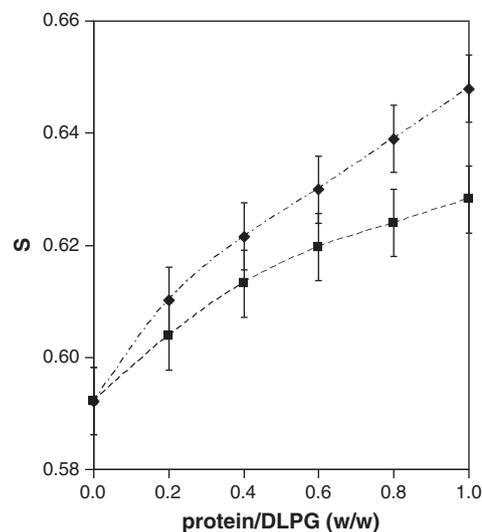

Fig. 5. Dependence of the 5-PCSL order parameter, S, in DLPG bilayers on the protein/lipid ratio for BS-RNase (full squares, dashed line) and G38K (full diamonds, dashed-dotted line).

in position 5, while at all other label positions a_N' variations are within the experimental uncertainty.

Fig. 4C shows that at each label position, the value of S is increased by the presence of proteins, *i.e.* the packing ordering increases and the rotational dynamics of the spin-labeled chains decreases upon interaction of both proteins with the membrane, the effect of G38K being bigger than that of the parent protein. Moreover, the bilayer surface is more perturbed than its interior. Indeed, in the case of BS-RNase, the S increase is almost undetectable already for the 10-PCSL, while for G38K a reduced, but still a significant S increase is observed up to the more internal spin label, 12-PCSL. However, we were not able to detect the appearance of a second, more motionally restricted component in the spectrum (see Fig. 4A), thus indicating that both BS-RNase and G38K do not penetrate deeply into the membrane interior [50], but remain confined to a quite external region of the bilayer although, in the case of G38K, perturbations due to the protein effectively propagate along the lipid acyl chains.

We also investigated the influence of the protein/lipid weight ratio on the order parameter of 5-PCSL in DLPG membranes, observing for both BS-RNase and G38K a continuous increase of S value (Fig. 5). This behavior is in contrast with the saturation trend usually observed for transmembrane proteins, or for proteins which steadily resides in the bilayer structure, thus suggesting a dynamic interaction, *i.e.*, a fast exchange regime between the proteins and the bilayer.

4. Conclusions

Knowledge of structural details that drive macromolecular recognition and interactions is essential not only to understand biological processes, but also to improve their efficiency and specificity in view of possible pharmacological applications. Based on these considerations, we have performed a careful study of the membrane interaction mechanism of BS-RNase, which represent a crucial aspect for its antitumor activity. We have also designed and characterized a BS-RNase variant with an increased toxic activity toward tumor cells by substituting a glycine residue on the protein surface with a basic residue. SPR and ESR studies on BS-RNase and its G38K variant point to a strong interaction of both enzymes, which are extremely basic proteins, with anionic phospholipid bilayers, mediated by a similar interaction mechanism. For both proteins, SPR data suggest a two-step process, composed by an initial binding to the bilayer surface, driven by electrostatic interactions, followed by an at least partial penetration in the lipid core. In turn, ESR data indicate that the

Fig. 4. (A) ESR spectra of n-PCSL in DLPG bilayer membranes, in the absence (continuous line) and presence of 1:1 (w/w) BS-RNase (dashed line) and G38K (dashed-dotted line) at 25 °C. The plot width is 90 G. (B) Dependence on spin-label position, n, of n-PCSL nitrogen hyperfine coupling constant, a_N', in DLPG bilayers, in the absence (open circles, continuous line) and presence of 1:1 (w/w) BS-RNase (full squares, dashed line), or G38K (full diamonds, dashed-dotted line). (C) Dependence on spin-label position, n, of n-PCSL order parameter, S, in DLPG bilayers, in the absence (open circles, continuous line) and presence of 1:1 (w/w) BS-RNase (full squares, dashed line), G38K (full diamonds, dashed-dotted line).

deepness of penetration is quite limited, both proteins remaining confined in the more external region of the bilayer microstructure. Despite the shallow insertion, the proteins effectively perturb the lipid packing and dynamics. In conclusion, our results, while ruling out the hypothesis that the protein crosses the membrane interior, support the hypothesis of a BS-RNase entry mediated by an endocytosis mechanism [51].

The comparison of SPR and EPR data show that with respect to BS-RNase G38K not only binds more strongly to the bilayer surface, but that the effects of protein-bilayer interaction more effectively propagate along the lipid acyl chains, perturbing the whole bilayer profile. Thus it can be concluded that the introduction of a lysine at position 38, by enhancing the protein-bilayer interaction, favors the BS-RNase translocation through membranes without altering the natural mechanism of the process.

This effect could well explain the increased cytotoxic activity of G38K with respect to the parent BS-RNase, although other concurring synergistic effects, notably a better resistance to RI of the monomeric derivative, which is supposed to be produced from the unswapped isoforms in the reducing cytosolic environment, cannot be completely excluded. However the substitution of glycine 38 with a basic residue is expected to play only a minor destabilizing effect, if any, on the putative complex of the monomeric BS-RNase with RI [44]. Furthermore, we would like to recall here that the swapped isoform of BS-RNase is already able to evade RI binding, even in the reducing cytosolic environment [16], whereas the monomeric derivative of BS-RNase, which represents the product of the less-abundant, unswapped isomer of BS-RNase in the same reducing conditions is inhibited from RI. These considerations lead us to conclude that the increased cytotoxic activity of G38K rely mainly on its better membrane interaction due to the presence of a positive charge cluster on the protein N-face, providing also a direct hint to design ribonucleases with even higher, selective, cytotoxic activity.

Supplementary materials related to this article can be found online at doi:10.1016/j.bbamem.2011.08.009.

Acknowledgements

References

[1] M. Inui, G. Martello, S. Piccolo, MicroRNA control of signal transduction, Nat. Rev. Mol. Cell Biol. 11 (2010) 252–263.
[2] W.C. Kim, C.H. Lee, The role of mammalian ribonucleases (RNases) in cancer, Biochim. Biophys. Acta 1796 (2009) 99–115.
[3] S.M. Rybak, M.A. Arndt, T. Schirrmann, S. Dubel, J. Krauss, Ribonucleases and immunoRNases as anticancer drugs, Curr. Pharm. Des. 15 (2009) 2665–2675.
[4] M. Los, New, exciting developments in experimental therapies in the early 21st century, Eur. J. Pharmacol. 625 (2009) 1–5.
[5] F. Leich, N. Stohr, A. Rietz, R. Ulbrich-Hofmann, U. Arnold, Endocytotic internalization as a crucial factor for the cytotoxicity of ribonucleases, J. Biol. Chem. 282 (2007) 27640–27646.
[6] T.J. Rutkoski, R.T. Raines, Evasion of ribonuclease inhibitor as a determinant of ribonuclease cytotoxicity, Curr. Pharm. Biotechnol. 9 (2008) 185–189.
[7] R.J. Youle, G. D'Alessio, Ribonucleases: Structures and Functions, Academic Press, NewYork, 1997.
[8] E. Boix, Y. Wu, V.M. Vasandani, S.K. Saxena, W. Ardelt, J. Ladner, R.J. Youle, Role of the N terminus in RNase A homologues: differences in catalytic activity, ribonuclease inhibitor interaction and cytotoxicity, J. Mol. Biol. 257 (1996) 992–1007.
[9] A. Di Donato, V. Cafaro, G. D'Alessio, Ribonuclease A can be transformed into a dimeric ribonuclease with antitumor activity, J. Biol. Chem. 269 (1994) 17394–17396.
[10] S. Di Gaetano, G. D'Alessio, R. Piccoli, Second generation antitumour human RNase: significance of its structural and functional features for the mechanism of antitumour action, Biochem. J. 358 (2001) 241–247.
[11] A. Antignani, M. Naddeo, M.V. Cubellis, A. Russo, G. D'Alessio, Antitumor action of seminal ribonuclease, its dimeric structure, and its resistance to the cytosolic ribonuclease inhibitor, Biochemistry 40 (2001) 3492–3496.
[12] P. Laccetti, D. Spalletti-Cernia, G. Portella, P. De Corato, G. D'Alessio, G. Vecchio, Seminal ribonuclease inhibits tumor growth and reduces the metastatic potential of Lewis lung carcinoma, Cancer Res. 54 (1994) 4253–4256.
[13] R. Piccoli, M. Tamburrini, G. Piccialli, A. Di Donato, A. Parente, G. D'Alessio, The dual-mode quaternary structure of seminal RNase, Proc. Natl. Acad. Sci. U. S. A. 89 (1992) 1870–1874.
[14] L. Mazzarella, S. Capasso, D. Demasi, G. Di Lorenzo, C.A. Mattia, A. Zagari, Bovine seminal ribonuclease: structure at 1.9 A resolution, Acta Crystallogr. D Biol. Crystallogr. 49 (1993) 389–402.
[15] R. Berisio, F. Sica, C. De Lorenzo, A. Di Fiore, R. Piccoli, A. Zagari, L. Mazzarella, Crystal structure of the dimeric unswapped form of bovine seminal ribonuclease, FEBS Lett. 554 (2003) 105–110.
[16] F. Sica, A. Di Fiore, A. Merlino, L. Mazzarella, Structure and stability of the non-covalent swapped dimer of bovine seminal ribonuclease: an enzyme tailored to evade ribonuclease protein inhibitor, J. Biol. Chem. 279 (2004) 36753–36760.
[17] C. Giancola, C. Ercole, I. Fotticchia, R. Spadaccini, E. Pizzo, G. D'Alessio, D. Picone, Structure-cytotoxicity relationships in bovine seminal ribonuclease: new insights from heat and chemical denaturation studies on variants, FEBS J. 278 (2011) 111–122.
[18] S.K. Saxena, S.M. Rybak, G. Winkler, H.M. Meade, P. McGray, R.J. Youle, E.J. Ackerman, Comparison of RNases and toxins upon injection into Xenopus oocytes, J. Biol. Chem. 266 (1991) 21208–21214.
[19] R.F. Turcotte, L.D. Lavis, R.T. Raines, Onconase cytotoxicity relies on the distribution of its positive charge, FEBS J. 276 (2009) 3846–3857.
[20] J. Matousek, G. Gotte, P. Pouckova, J. Soucek, T. Slavik, F. Vottariello, M. Libonati, Antitumor activity and other biological actions of oligomers of ribonuclease A, J. Biol. Chem. 278 (2003) 23817–23822.
[21] E. Notomista, J.M. Mancheno, O. Crescenzi, A. Di Donato, J. Gavilanes, G. D'Alessio, The role of electrostatic interactions in the antitumor activity of dimeric RNases, FEBS J. 273 (2006) 3687–3697.
[22] J.M. Mancheno, M. Gasset, M. Onaderra, J.G. Gavilanes, G. D'Alessio, Bovine seminal ribonuclease destabilizes negatively charged membranes, Biochem. Biophys. Res. Commun. 199 (1994) 119–124.
[23] N. Eswar, B. Webb, M.A. Marti-Renom, M.S. Madhusudhan, D. Eramian, M.Y. Shen, U. Pieper, A. Sali, Comparative protein structure modeling using modeller, Curr. Protoc. Bioinformatics Chapter 5 (2006) Unit 5 6.
[24] A. Fiser, R.K. Do, A. Sali, Modeling of loops in protein structures, Protein Sci. 9 (2000) 1753–1773.
[25] R. Koradi, M. Billeter, K. Wuthrich, MOLMOL: a program for display and analysis of macromolecular structures, J. Mol. Graph. 14 (1996) 51–55 29–32.
[26] W.L. DeLano, The PyMOL Molecular Graphics System, DeLano Scientific, Palo Alto, CA, USA, 2002.
[27] W. Rocchia, E. Alexov, B. Honig, Extending the applicability of the nonlinear Poisson-Boltzmann equation: multiple dielectric constants and multivalent ions, J. Phys. Chem. B 105 (28) (2001) 6507–6514.
[28] A. Di Donato, G. D'Alessio, Heterogeneity of bovine seminal ribonuclease, Biochemistry 20 (1981) 7232–7237.
[29] A. Di Donato, P. Galletti, G. D'Alessio, Selective deamidation and enzymatic methylation of seminal ribonuclease, Biochemistry 25 (1986) 8361–8368.
[30] F. Avitabile, C. Alfano, R. Spadaccini, O. Crescenzi, A.M. D'Ursi, G. D'Alessio, T. Tancredi, D. Picone, The swapping of terminal arms in ribonucleases: comparison of the solution structure of monomeric bovine seminal and pancreatic ribonucleases, Biochemistry 42 (2003) 8704–8711.
[31] C. Ercole, R. Spadaccini, C. Alfano, T. Tancredi, D. Picone, A new mutant of bovine seminal ribonuclease with a reversed swapping propensity, Biochemistry 46 (2007) 2227–2232.
[32] M. Kunitz, A spectrophotometric method for the measurement of ribonuclease activity, J. Biol. Chem. 164 (1946) 563–568.
[33] M. Tamburrini, R. Piccoli, D. Picone, A. Di Donato, G. D'Alessio, Dissociation and reconstitution of bovine seminal RNAase: construction of a hyperactive hybrid dimer, J. Protein Chem. 8 (1989) 719–731.
[34] C. Ercole, F. Avitabile, P. Del Vecchio, O. Crescenzi, T. Tancredi, D. Picone, Role of the hinge peptide and the intersubunit interface in the swapping of N-termini in dimeric bovine seminal RNase, Eur. J. Biochem. 270 (2003) 4729–4735.
[35] B.S. Adinolfi, V. Cafaro, G. D'Alessio, A. Di Donato, Full antitumor action of recombinant seminal ribonuclease depends on the removal of its N-terminal methionine, Biochem. Biophys. Res. Commun. 213 (1995) 525–532.
[36] K. Abe, H. Kimura, Amyloid beta toxicity consists of a Ca(2+)-independent early phase and a Ca(2+)-dependent late phase, J. Neurochem. 67 (1996) 2074–2078.
[37] E. Gazit, W.J. Lee, P.T. Brey, Y. Shai, Mode of action of the antibacterial cecropin B2: a spectrofluorometric study, Biochemistry 33 (1994) 10681–10692.
[38] H. Mozsolits, W.G. Thomas, M.I. Aguilar, Surface plasmon resonance spectroscopy in the study of membrane-mediated cell signalling, J. Pept. Sci. 9 (2003) 77–89.
[39] T.A. Morton, D.G. Myszka, I.M. Chaiken, Interpreting complex binding kinetics from optical biosensors: a comparison of linear analysis, the integrated rate equation and numerical integration, Anal. Biochem. 227 (1995) 176–185.

[40] G. D'Errico, A.M. D'Ursi, D. Marsh, Interaction of a peptide derived from glycoprotein gp36 of feline immunodeficiency virus and its lipoylated analogue with phospholipid membranes, Biochemistry 47 (2008) 5317–5327.

[41] L.M. Gordon, C.C. Curtain, Electron spin resonance analysis of model and biological membranes, in: R.C. Aloia, C.C. Curtain, L.M. Gordon (Eds.), Advances in Membrane Fluidity: Methods for Studying Membrane Fluidity, vol. 1, Alan R. Liss, New York, 1988, pp. 25–89.

[42] G. D'Errico, G. Vitiello, O. Ortona, A. Tedeschi, A. Ramunno, A.M. D'Ursi, Interaction between Alzheimer's Abeta(25–35) peptide and phospholipid bilayers: the role of cholesterol, Biochim. Biophys. Acta 1778 (2008) 2710–2716.

[43] J.E. Lee, R.T. Raines, Cytotoxicity of bovine seminal ribonuclease: monomer versus dimer, Biochemistry 44 (2005) 15760–15767.

[44] B. Kobe, J. Deisenhofer, Mechanism of ribonuclease inhibition by ribonuclease inhibitor protein based on the crystal structure of its complex with ribonuclease A, J. Mol. Biol. 264 (1996) 1028–1043.

[45] N. Papo, Y. Shai, Exploring peptide membrane interaction using surface plasmon resonance: differentiation between pore formation versus membrane disruption by lytic peptides, Biochemistry 42 (2003) 458–466.

[46] Y. Shai, Mechanism of the binding, insertion and destabilization of phospholipid bilayer membranes by alpha-helical antimicrobial and cell non-selective membrane-lytic peptides, Biochim. Biophys. Acta 1462 (1999) 55–70.

[47] S. Galdiero, A. Falanga, G. Vitiello, M. Vitiello, C. Pedone, G. D'Errico, M. Galdiero, Role of membranotropic sequences from herpes simplex virus type I glycoproteins B and H in the fusion process, Biochim. Biophys. Acta 1798 (2010) 579–591.

[48] S. Galdiero, A. Falanga, M. Vitiello, L. Raiola, L. Russo, C. Pedone, C. Isernia, M. Galdiero, The presence of a single N-terminal histidine residue enhances the fusogenic properties of a Membranotropic peptide derived from herpes simplex virus type 1 glycoprotein H, J. Biol. Chem. 285 (2010) 17123–17136.

[49] D. Marsh, Electron spin resonance in membrane research: protein–lipid interactions, Methods 46 (2008) 83–96.

[50] M.B. Sankaram, P.J. Brophy, D. Marsh, Spin-label ESR studies on the interaction of bovine spinal cord myelin basic protein with dimyristoylphosphatidylglycerol dispersions, Biochemistry 28 (1989) 9685–9691.

[51] M.C. Haigis, R.T. Raines, Secretory ribonucleases are internalized by a dynamin-independent endocytic pathway, J. Cell Sci. 116 (2003) 313–324.